Chapter 5
Simulation of Modal Survey Using Direct Field Acoustic Noise as Inputs

Kevin Napolitano and Dr. Michael Yang

Abstract Direct field acoustic noise (DFAN) testing involves mounting several sets of acoustic sources around a structure to provide inputs for acoustic qualification tests. It is becoming more prevalent because it is often less expensive than traditional reverberant chamber testing while also allowing acoustic tests to be performed at the test article facility, which reduces or eliminates test article transportation costs. This effort discusses the ability of acoustic analysis software packages to simulate acoustic modal survey tests so that the viability of using DFAN sources can be assessed well before a modal survey test is conducted.

Keywords Modal testing ·Parameter estimation ·Direct field acoustic noise ·Pretest analysis

Introduction

Direct field acoustic noise (DFAN) acoustic environmental testing involves placing a number of acoustic sources, usually a set of large speakers that together cover the acoustic frequency range of interest, around a structure and then controlling their excitation levels to meet required acoustic levels for the test.

DFAN testing has been gaining popularity as a way to perform acoustic environmental tests on structures when it saves a program schedule and budget compared to testing in a reverberant chamber. Further schedule and budget could be saved if DFAN sources could also be used as exciters in modal survey tests.

The objective of this paper is to perform pretest analysis on a finite element model (FEM) using acoustic sources as inputs. The FEM and acoustic source models were used to model the test setup of a demonstration article [1], shown in Fig. 1. Twelve Acoustic Research Systems (ARS) Neutron speaker systems are, in stacks of two, are evenly placed in a

Fig. 1 Demonstration article inside 6 × 2 configuration of ARS Neutron acoustic sources.

Kevin Napolitano · Dr. Michael Yang
ATA Engineering, Inc., San Diego, California, 92128, USA
e-mail: kevin_napolitano@yahoo.com; myang@ata-e.com

© The Author(s), under exclusive license to River Publishers 2025

Brandon Dilworth et al. (eds.), *Topics in Modal Analysis & Parameter Identification I, Vol. 9*, Conference Proceedings of the Society for Experimental Mechanics Series, https://doi.org/10.13052/97887-438-0154-2_5

circle around the test article. Twelve control microphones are mounted, one in front of each speaker, to control speaker output to a predefined output level. This demonstration test was performed at Experior Laboratories in Oxnard, California, using a Neutron DFAN system provided by ARS.

This paper describes the NASTRAN FEM, modeling of the acoustic sources using Wave6 vibroacoustic analysis software, and processing of the analysis results to determine which modes are observable from the acoustic inputs and highlights some issues that may need to be accounted for during a modal survey test.

Baseline Nastran Model

The test article simulates a spacecraft on the head expander of a vertical base shaker. The FEM and test display model of the test article are shown in Fig. 2. The isolators between the base plate and the sawhorses represent the airbags used to keep the head expander at a specific height under load, and the sawhorses represent the complicated dynamics of the shaker table system.

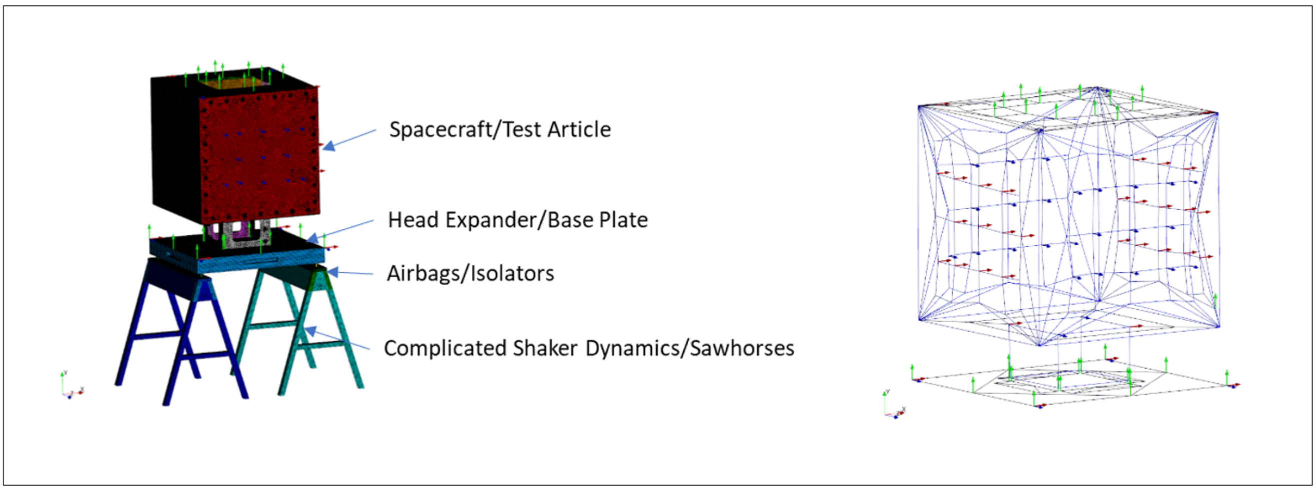

Fig. 2 FEM (left) and test display model (right) showing accelerometer locations.

The FEM includes the demonstration article, its rubber isolators at the base, and the sawhorses used to support the test article at an optimal height for the acoustic sources. The FEM has approximately 230,000 elements and 236,000 nodes. The rubber isolators are represented with spring elements.

The objectives of the pretest analysis were to 1) select sensors to measure all test article modes up to 100 Hz (with the exception of local sawhorse modes, which were decoupled from the test article due to the isolators), 2) measure the base at the bottom of the test article, and 3) locate enough accelerometers to observe the six rigid body deformations as well as the first flexible mode of the base. To this end, 94 test degrees of freedom (DOFs) were selected using engineering judgement and conventional sensor up-selection and down-selection algorithms [1]. Static condensation (i.e., Guyan reduction) of the mass and stiffness matrices down to these test locations was then performed, and the 94-DOF mass matrix was used in the following orthogonality calculations.

Ideally, for aerospace modal tests the off-diagonal terms of the self-orthogonality matrix during pretest analysis are minimized as much as practicable. For this analysis, the majority of the off-diagonal terms were under 5%, with the maximum off-diagonal value being 9%. While these results may not be acceptable for some modal survey tests, they were good enough that the modes could be observed and differentiated from each other.

Acoustic Source Modeling

A simulation of a DFAN test with a 2×6 configuration of ARS Neutron speakers was performed using Wave6. A FEM of the test article was imported into Wave6 as finite element (FE) subsystem. The fluid (air) and speaker loading were simulated with the boundary element method (BEM). The calibrated Neutron speaker sources were not directly used because the

Table 1 FEM self-orthogonality matrix.

FEM Self Orthogonality Table

FEM Shapes		1	2	3	4	5	6	7	8	9	10	11	12	13	14	15	16	17	18	19	20	21	22	23	24	25	26	27	28	29	30	31	32	33	34	35
		3.84	3.91	6.06	6.20	6.90	8.78	17.82	19.97	20.26	23.02	25.06	27.39	27.58	42.64	44.02	47.51	48.85	50.43	53.23	54.29	58.79	61.14	62.94	65.28	75.35	76.58	80.91	84.34	87.57	87.67	90.96	93.74	95.16	99.43	100.43
1	3.84	100																																		
2	3.91		100																																	
3	6.06			100																																
4	6.20				100																															
5	6.90					100																														
6	8.78						100																													
7	17.82							100																												
8	19.97								100																											
9	20.26									100																										
10	23.02										100																									
11	25.06											100																								
12	27.39												100																							5
13	27.58													100																						
14	42.64														100																				5	7
15	44.02															100										5										
16	47.51																100									7										
17	48.85																	100									7									6
18	50.43																		100																	
19	53.23																			100																
20	54.29																				100															
21	58.79																					100							5							
22	61.14																						100			5										
23	62.94																							100												
24	65.28																								100											
25	75.35															5	7						5			100										
26	76.58																	7									100								8	
27	80.91																											100							5	
28	84.34																					5							100							
29	87.57																													100						
30	87.67																														100					
31	90.96																															100		5		
32	93.74																																100			
33	95.16																															5		100		
34	99.43														5												8	5							100	9
35	100.43											5			7			6																	9	100

version of Wave6 at the time of this writing only allowed for random analysis using those sources. Instead, rigid fluid surfaces were used to represent the fronts of the stacked speakers. These are idealized surfaces with effectively infinite impedance that will reflect incoming sound waves perfectly (i.e., without loss or distortion). A single monopole was placed at the center of each speaker face. Virtual microphones were placed in locations corresponding to those in the test configuration. Fig. 3

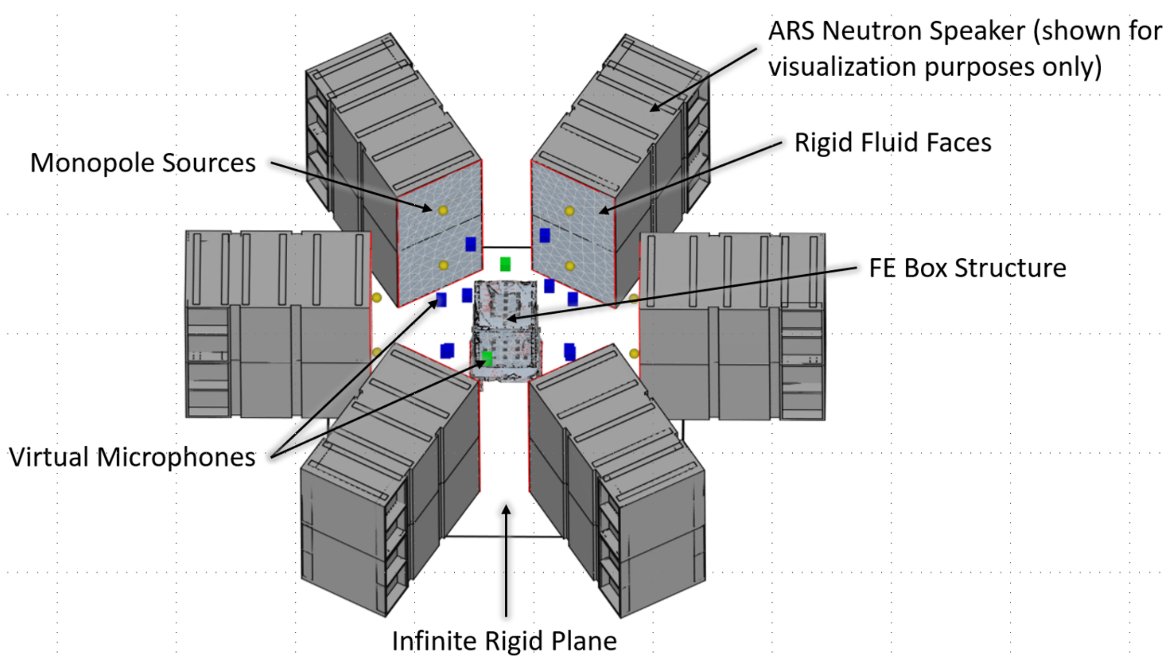

Fig. 3 Wave6 FE/BEM model (with ARS Neutron speakers shown for visualization purposes only). The blue and green squares represent control and monitor microphones, respectively.

illustrates the Wave6 model with the ARS Neutrons shown for visualization purposes. However, since these speaker sources were not explicitly used in the analysis, Fig. 4 is a more accurate representation of the fluid surfaces in the model.

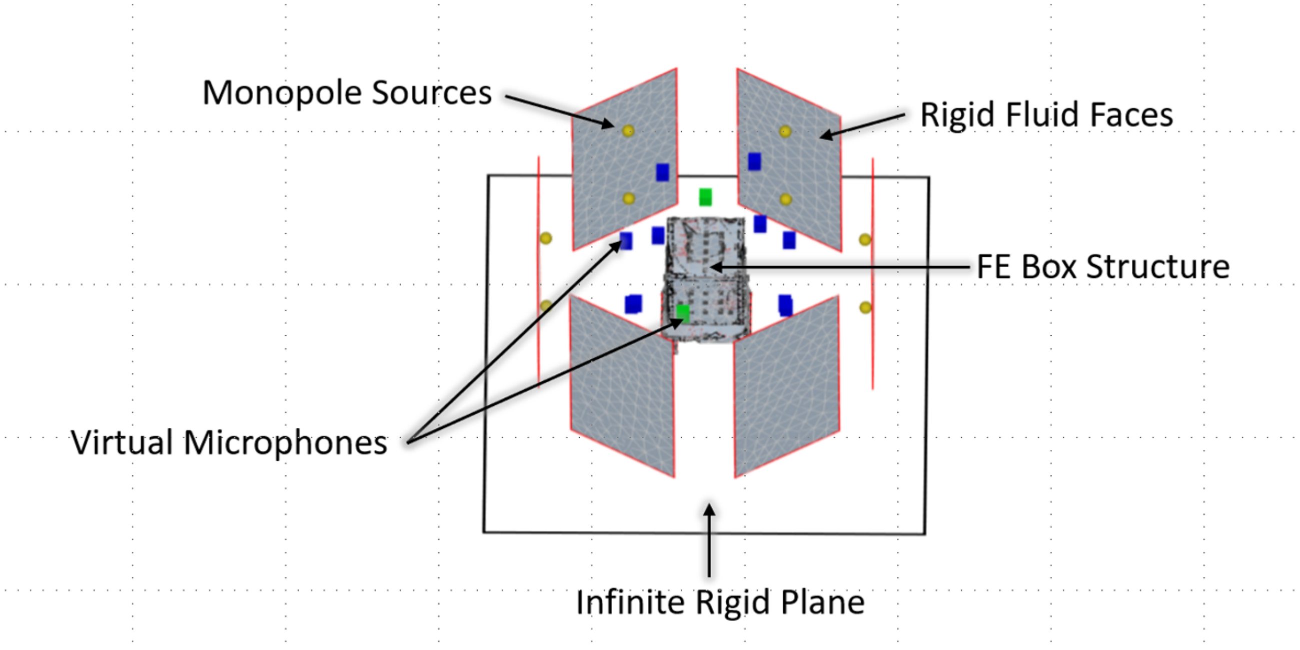

Fig. 4 Wave6 FE/BEM model with all structural and fluid components shown.

A separate load case was defined for each of the twelve monopole sources. Each monopole source was defined to have a sound power of 1+0i lbf-in/s at all frequencies. The model was solved deterministically from 1 to 367 Hz in 0.05 Hz increments. The frequency spacing was chosen for convenience and to match the spacing from the test. The structural FEM was given a structural damping loss factor of 1.0% at all frequencies, which corresponds to a 0.5% viscous damping value. The following responses were recovered:

- Acceleration (y) responses at 88 nodes on the FEM which correspond to the accelerometer locations on the physical test article. All translations were recovered in the global (CS 0) coordinate system.
- The modal amplitudes (q) for each of the structural modes.
- The field pressure (p) at the virtual microphone locations.

The results for each load case are placed in a column vector such that the response for all twelve load cases are $[y]$, $[q]$, and $[p]$, where the rows of each matrix correspond to their respective DOFs and the columns are associated with each load case.

Since each source consisted of a unit input, the output responses $[y]$, $[q]$, and $[p]$, are equal to their respective frequency response function (FRF) matrices $[H_{ys}]$, $[H_{qs}]$, and $[H_{ps}]$, where the subscript s refers to the acoustic sources. The microphone responses can be partitioned to the control microphones, $[c]$, which is also the FRF matrix associated with the control microphones $[H_{cs}]$.

All results were exported in HDF5 format and then imported into MATLAB for further processing in ATA's IMAT$^{\mathrm{TM}}$ software.

The modal amplitudes were used to calculate $[S_{qq}]$, the modal cross-spectral density matrix. This is a square matrix with the number of rows and columns equal to the number of *in vacuo* structural modes (i.e., structural modes that are not influenced by the surrounding fluid). It represents the random contribution of the structural modes at each frequency if each monopole source was used to excite the structure in an uncorrelated manner. $[S_{qq}]$ at each analysis frequency is calculated as

$$[S_{qq}] = [H_{qs}]\,[S_{ss}]\,[H_{qs}]^{H},$$

where $[S_{ss}]$ is the identity matrix because each monopole has unit input and is assumed to be uncorrelated from the other monopoles. The superscript H denotes the Hermitian, or complex conjugate transpose. The diagonal of $[S_{qq}]$ can be plotted as a function of frequency to estimate how efficiently each structural mode is excited, as shown in Fig. 5.

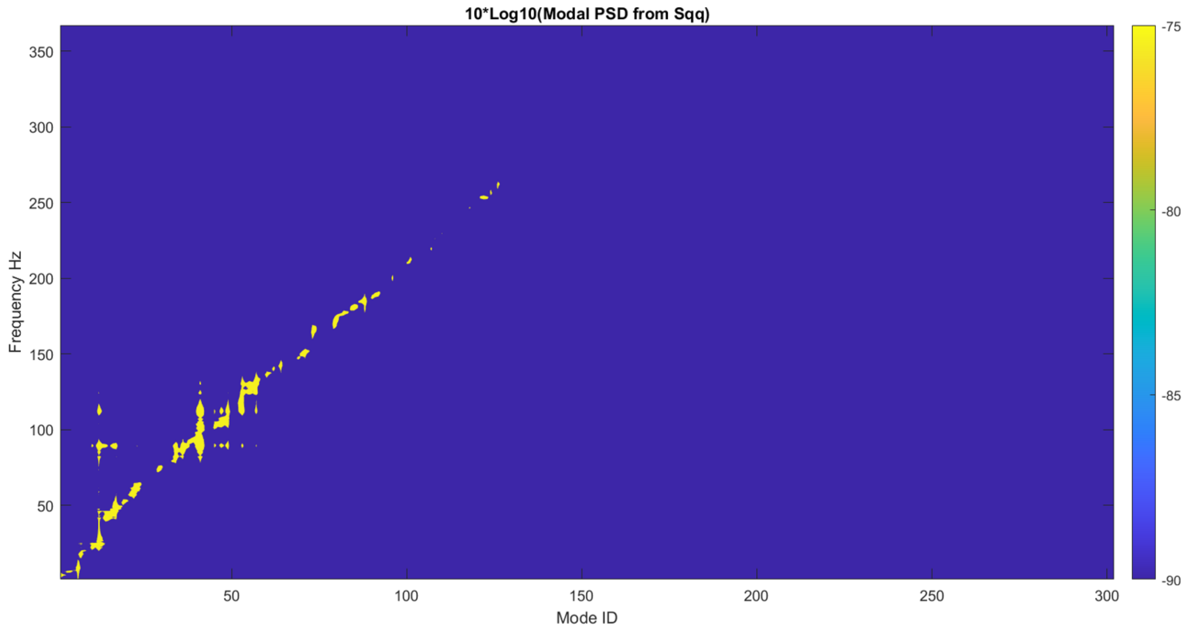

Fig. 5 Diagonal of $[S_{qq}]$ as a function of frequency.

The cross-spectral density matrix of physical responses, $[S_{yy}]$, can be calculated from $[S_{qq}]$ as

$$[S_{yy}] = [\Phi]\,[S_{qq}]\,[\Phi]^H, \tag{1}$$

where $[\Phi]$ represents the modal matrix with modal vectors organized into columns. This formulation allows recovery of any structural response for which modes can be supplied.

Test Simulation

The objective of simulating acoustic excitation is to better understand the validity of extracting modes from acoustically excited test articles. Specifically, the objective is to determine 1) which mode shapes the acoustic system should excite and 2) which apparent modes that may appear in the test data which are not actual structural modes.

For this paper, the sources are analytically defined to be equal to 1 mPa/Hz^2 over all frequencies. This differs from an acoustic test because 1) acoustic excitation sources typically roll off at frequencies below 20–30 Hz and 2) in test, the excitation levels are used to set levels certain levels over 1/n frequency bands. Future analysis efforts should also include the control algorithm used for setting exciter levels.

The matrix $[S_{yy}]$ was calculated two ways using the FRF matrices. The first way assumes that the sources are uncontrolled and constant as a function of frequency. Unfortunately, the sources cannot be measured directly, so the second way calculates it assuming that the control microphones were uncorrelated and set to 1 mPa/Hz^2. The second calculation was done by assuming the control microphone levels were set at each frequency by inverting the $[H_{cs}]$ and then postmultiplying the $[H_{ys}]$ matrix to generate an FRF matrix associated with microphones as references, such that

$$[H_{yc}] = [H_{ys}]\,[H_{cs}]^{-1}. \tag{2}$$

It should be noted that this is *not* how the control microphones levels are set, but performing this calculation can lead to insight into the pretest analysis. Future effort on modeling the control algorithm directly should be a priority.

The $[H_{yc}]$ matrix can be measured directly in test and was also investigated as a way to solve for modes. To do so, it was used to simulate the $[S_{yy}]$ assuming the $[S_{cc}]$ was equal to the identity matrix and then comparing it to the original $[S_{yy}]$ matrix that assumes $[S_{ff}]$ matrix was equal to the identity matrix.

Modal Extraction

The operational modal analysis technique described in [2] was used to extract modes from the simulated test data assuming $[S_{ff}]$ was equal to the identify matrix. The full 94 $\times$ 94 $[S_{yy}]$ matrix was fed into ATA's OPoly modal analysis tool and then the following procedure was performed over a series of frequency bands from 0 to 101 Hz.

1. Virtual references were calculated over small frequency bands of closely spaced modes by performing singular value decomposition of the $[S_{yy}]$ matrix.
2. The columns of the $[S_{yy}]$ matrix were reduced to these virtual references, shrinking the matrix from 94 $\times$ 94 to the number of modes in the frequency range (typically 1 to 4).
3. Real modes were solved and exported.

Once completed, the test simulated modes were compared to the original modes from NASTRAN.

The simulated test self-orthogonality matrix is presented in Table 2. Off-diagonal values are higher than what would be typical for a modal test. This is most likely due to the fact that the panels of the test article are very susceptible to the effects of air mass because they are light, flexible, and have large surface areas. Typically, the self-orthogonality matrix is used to help debug the test setup, as large off-diagonals are often associated with inaccurate modal extractions due to modes being poorly excited or not well differentiated with other closely spaced modes, or errors in the channel table. If the added air mass is not accounted for in the model, then other methods of verifying the shape extractions, such as viewing animated modes shapes or overlaying test data with simulated data synthesized from the modal parameters must be performed during an actual test.

Table 2 Simulated acoustic structural test modes – self-orthogonality matrix.

Test Self Orthogonality Table

Test Shapes

Simulated		1	2	3	4	5	6	7	8	9	10	11	12	13	14	15	16	17	18	19	20	21	22	23	24	25	26	27	28	29	30
Test Shapes		3.80	3.87	6.05	6.18	8.74	17.71	22.11	24.12	24.62	26.44	41.71	43.04	46.09	47.42	49.17	51.98	52.86	56.97	59.16	61.37	63.85	73.76	82.30	85.53	86.28	89.31	89.50	91.81	93.57	98.07
1	3.80	100																													
2	3.87		100																												
3	6.05			100																											
4	6.18				100																										
5	8.74					100																									
6	17.71						100		39	14																					
7	22.11							100		7																6	14	6			
8	24.12						39		100	25													5			7	24	7			
9	24.62						14	7	25	100														7	5	9	34	8			6
10	26.44										100																				
11	41.71											100																			
12	43.04												100																		
13	46.09													100	16								6				10				
14	47.42													16	100	5											6				
15	49.17														5	100															
16	51.98																100	20													
17	52.86																20	100													
18	56.97																		100	7											
19	59.16																		7	100	10										
20	61.37																			10	100	6					5				
21	63.85																				6	100									
22	73.76								5					6									100	7	5		5		5		
23	82.30									7													7	100	19		18				
24	85.53									5													5	19	100	29	20	35			
25	86.28							6	7	9															29	100	41	42			
26	89.31							14	24	34				10	6						5		5	18	20	41	100	52		11	6
27	89.50							6	7	8															35	42	52	100		9	
28	91.81																						5						100	29	8
29	93.57																										11	9	29	100	8
30	98.07									6																	6		8	8	100

The cross-orthogonality matrix between the simulated test modes (rows) and the NASTRAN FEM shapes (columns) is shown in Table 3. The NASTRAN modes that were not extracted are highlighted in pink. The high values in the Test CRSS columns show that each simulated test mode is a mass-weighted, linear combination of the FEM shapes. All simulated test modes are captured by the FEM shapes with the exception of mode 26, which is best mapped by a FEM mode just above 100 Hz. The CRSS rows show how much of each FEM shape is captured by the simulated test shapes. FEM modes 4, 8, 9, 26, and 27 were not extracted because the acoustic sources did not excite them adequately enough to obtain good modal parameters. Note that damping levels are almost twice the nominal value for simulated test mode 26. The differences in damping could be due to structure/air interaction that is independent of excitation source, or it could be due to the excitation source interacting with the test article.

Table 3 Acoustic structural modes using in vacuo mass matrix – baseline FEM modes cross-orthogonality matrix.

			FEM/Simulated Test Cross Orthogonality Table																																				
Simulated Test			FEM Shapes																																			Test	Test
	Freq	Damp	1	2	3	4	5	6	7	8	9	10	11	12	13	14	15	16	17	18	19	20	21	22	23	24	29	30	33	34	35	36	37	38	39	40	41	CRSS	CRSS
No.	Hz	%crit	3.84	3.91	6.06	6.20	6.90	8.78	17.82	19.97	20.26	23.02	25.06	27.39	27.58	42.64	44.02	47.51	48.85	50.43	53.23	54.29	58.79	61.14	62.94	65.28	75.35	76.58	80.91	84.34	87.57	87.67	90.96	93.74	95.16	99.43	100.43	3%	All
1	3.80	0.50	100																																			100	100
2	3.87	0.50		100																																		100	100
3	6.05	0.50			100																																	100	100
4	6.18	0.50				100																																100	100
5	8.74	0.50						100																														100	100
6	17.71	0.50							89				46																									89	100
7	22.11	0.50										99																										99	100
8	24.12	0.51											86	48																								86	100
9	24.62	0.49											28	90	26																							94	100
10	26.44	0.51												28	96																							100	100
11	41.71	0.51														100																						100	100
12	43.04	0.51															100																					100	100
13	46.09	0.51																98																				99	100
14	47.42	0.52																30	95																			100	100
15	49.17	0.51																		99																		99	100
16	51.98	0.51																			99																	100	100
17	52.86	0.51																				99																100	100
18	56.97	0.51																					100															100	100
19	59.16	0.52																						99														100	100
20	61.37	0.52																							99													99	100
21	63.85	0.52																								99												99	100
22	73.76	0.51																									100											100	100
23	82.30	0.55																												99								99	100
24	85.53	0.56																													37	92						99	100
25	86.28	0.52																													74	61						96	100
26	89.31	1.12												37																27		30	25				65	70	97
27	89.50	0.58																														39	90				20	90	100
28	91.81	0.60																																99				99	100
29	93.57	0.53																																26	92			96	100
30	98.07	0.52																																		95	34	98	100
CRSS	3%		100	100	100	100	1	100	89	3	3	99	100	94	96	100	100	99	99	99	100	100	100	99	99	99	100	9	7	99	96	98	93	99	96	95	68		
CRSS	All		100	100	100	100	2	100	100	4	4	100	100	100	100	100	100	100	100	100	100	100	100	100	100	100	100	16	14	100	100	100	100	100	100	99	90		

A plot of the first three singular values of the $[S_{yy}]$ matrix with red boxes around the frequencies of the unextracted modes is shown in Fig. 6. Peaks in the singular values can be seen for most of these modes, but they are not as pronounced as they are with the other modes, and the authors believe that the modes would not be accurately extracted if there were any reasonable level of noise in the test data. These results are similar to those from almost any modal test that uses modal shakers as the input source, and the solution is to perform another test in which those modes are excited directly.

The singular values of the control microphone cross spectrum matrix are shown in Fig. 7. The local minima in this matrix (indicated by the vertical cursors) can potentially lead to fictitious modes if microphones are used as references when calculating FRF. The peaks in the FRF are likely due to an acoustic node coinciding with the microphone locations at these frequencies.

An overlay of the three primary singular values for constant source input and constant microphone input are presented in Fig. 8. The two peaks near 87 and 121 Hz in the microphone-generated singular values correspond to the local minima in Fig. 7 and are not actual modes, but the mode near 110 Hz looks very similar to the apparently heavily damped peak evident in the source singular values.

One way to verify whether the changes in damping are due to the structure interacting with air or the excitation source is to excite the modes directly with a non-acoustic source. This will eliminate any damping changes due to the source.

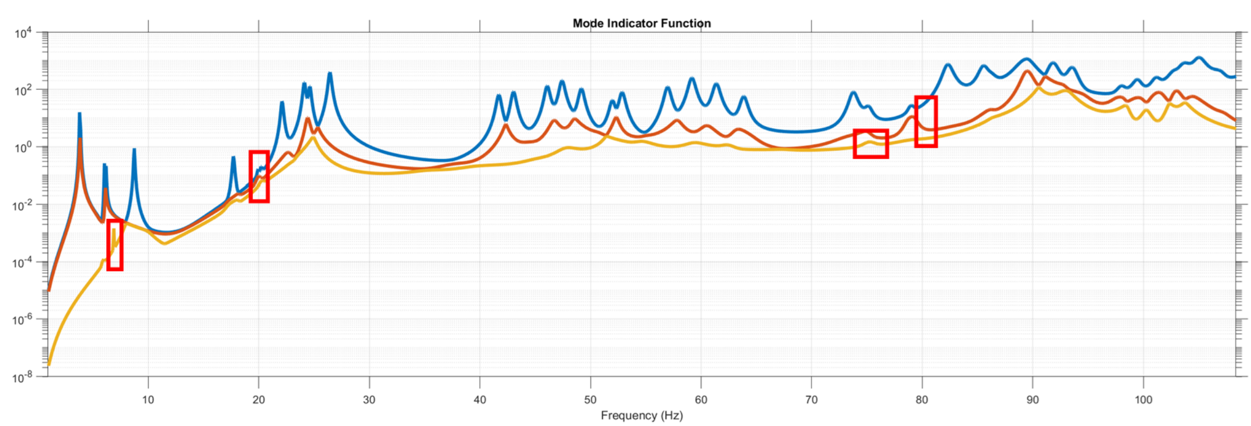

Fig. 6 Singular values of acceleration cross spectrum matrix. Acoustically insensitive modes are identified inside red boxes.

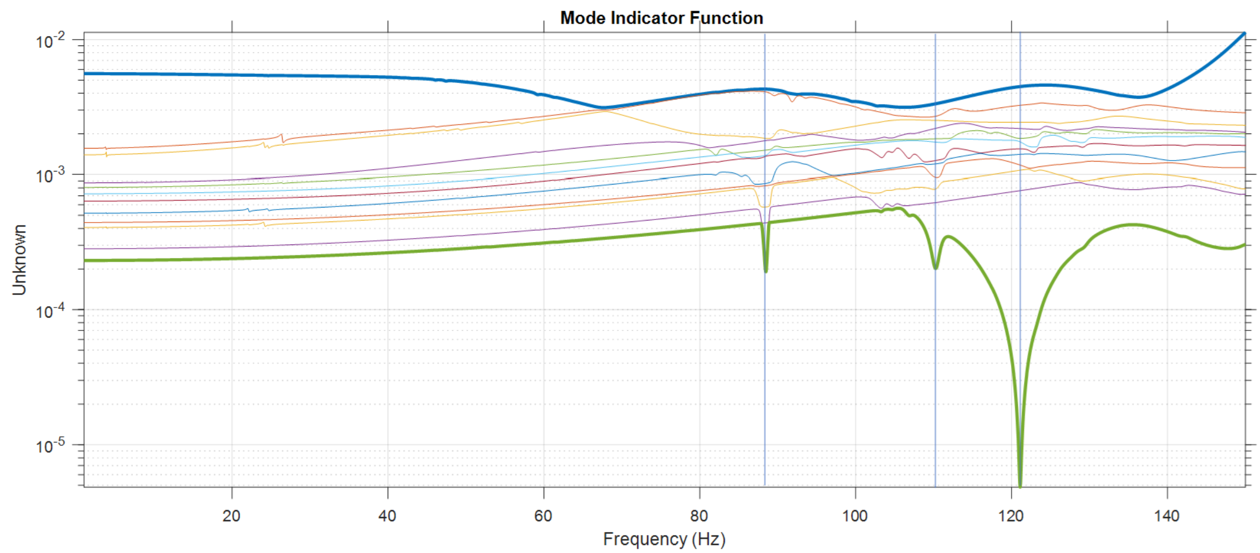

Fig. 7 Singular values of control microphone cross spectrum matrix.

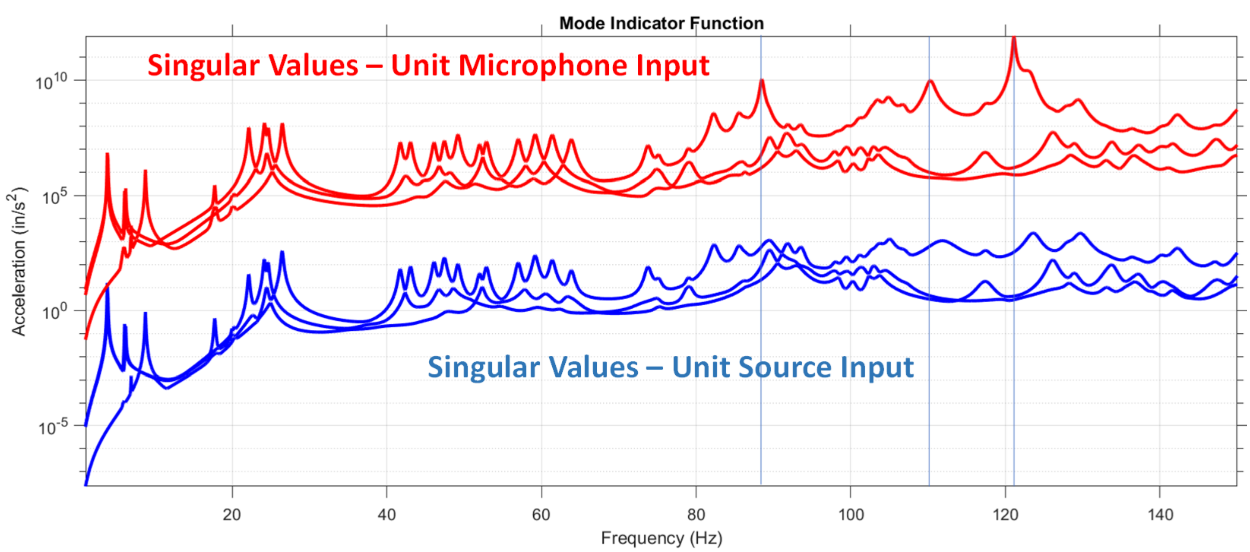

Fig. 8 Singular values of $[S_{yy}]$ due to unit source input and unit control microphone input.

Summary and Observations

The pretest analysis in this paper shows that modes can be extracted from acoustic tests. As with any modal survey test, using conventional sensor selection algorithms for placing accelerometers is sufficient even when the excitation source is acoustic. However, for acoustically sensitive structures, the effects of air mass should be included if test self-orthogonality matrices are used as a test exit criterion. That said, the baseline mass matrix should be sufficient for test-FEM cross orthogonality comparisons.

As with most modal survey tests, the input sources may not excite all of the modes of interest. In these cases, plans should be made to excite those modes by other means. Likewise, test results showing that there are duplicate modes extracted at different frequencies, likely due to zeros in the microphone/source FRF, should also be verified by exciting those modes directly by other means.

The changes in modal damping are due to either interaction between the structure and air mass or the way the source interacts with the system.

In this work, a comparison between the modal extractions from acoustic excitation and modes calculated without acoustic effects incorporations was presented. Therefore it was difficult to determine whether changes in modal parameters such as damping were due to frequency variation of the acoustic input loads or to the structure residing in fluid air. Thus, future work should include a comparison of modal extractions to the modes associated with the wet structure.

References

1. Napolitano, K., Yang, M., Friedlander, E., and Schick, D., "Mode Shape Extraction Using Direct Field Acoustic Noise Test Data," *43rd International Modal Analysis Conference*, February 10–13, 2025.
2. Flanigan, C., and Botos, D., "Automated Selection of Accelerometer Locations for Modal Survey Tests," *10th International Modal Analysis Conference*, San Diego, California, February 3–6, 1992.
3. Crowley, J.R., Klosterman, A.L., Rocklin, G.T., and Vold, H., "Direct Structural Modification Using Frequency Response Functions," *Proceedings of the Second International Modal Analysis Conference*, Orlando, Florida, February 1984, pp. 58–65.
4. Fladung, W.A., "Why Don't We Just Use the Cross Spectra for Operational Modal Analysis?" *43rd International Modal Analysis Conference*, February 10–13, 2025.